Final Report for AFOSR Project

March 19, 2007

Title

Synthesis and modulation of visible-bandgap semiconductor nanowires and their optical sensor application

Research Period: 2006. 1. 1 ~ 2006. 12. 31

Principal Investigator: Dr. Kyoung-Jin Choi

- e-mail address: kjchoi@kist.re.kr
- Institution: Nano-Science Research Division, Korea Institute of Science and Technology (KIST)
- Mailing Address: Nano-materials Research Center, KIST, Sungbuk, Seoul, 136-791, Korea
- Phone: 82-2-958-5502
- Fax: 82-2-958-5509

Co-Investigators:

Dr. Jae-Gwan Park: Principal Research Scientist, Division of Materials, KIST

Dr. Jae-Hwan Park: Assistant Professor, College of Electrical Electronic and Information Engineering, Chungju National University

Mr. Seok-Joon Kwon: Research Scientist, Division of Materials, KIST

Project Summary

Research Goal	Research Contents
Synthesis and modulation of visible bandgap semiconductor NWs	- Synthesis and shape control of CdS, CdSe, and CdS-Se NWs using PLD - Modulation of bandgap energy using CdS-Se in the visible range
Realization of NW-based optical sensor	- Measurements of opto-electronic properties of visible-range optical sensor

Budget Summary

(1) Salaries US$ 25,000 (Internal Salaries should be 25% against total budget)

(2) Equipment US$ 20,000

(3) Consumable materials US$ 25,000

Report Documentation Page

Form Approved
OMB No. 0704-0188

1. REPORT DATE	2. REPORT TYPE	3. DATES COVERED
12 MAY 2007	**FInal**	**28-02-2006 to 20-03-2007**

4. TITLE AND SUBTITLE
Synthesis and modulation of visible-bandgap semiconductor nanowire and their optical sensor application

5a. CONTRACT NUMBER
FA520906P0165

5b. GRANT NUMBER

5c. PROGRAM ELEMENT NUMBER

6. AUTHOR(S)
Jae Hwan Park

5d. PROJECT NUMBER

5e. TASK NUMBER

5f. WORK UNIT NUMBER

7. PERFORMING ORGANIZATION NAME(S) AND ADDRESS(ES)
Korea Institute of Science and Technology,39-1, Haweolgok-dong, Sungbuk-ku,Seoul 136-791,Korea (South),KR,136-791

8. PERFORMING ORGANIZATION REPORT NUMBER
N/A

9. SPONSORING/MONITORING AGENCY NAME(S) AND ADDRESS(ES)
AOARD, UNIT 45002, APO, AP, 96337-5002

10. SPONSOR/MONITOR'S ACRONYM(S)
AOARD

11. SPONSOR/MONITOR'S REPORT NUMBER(S)
AOARD-064016

12. DISTRIBUTION/AVAILABILITY STATEMENT
Approved for public release; distribution unlimited

13. SUPPLEMENTARY NOTES

14. ABSTRACT
The work successfully demonstrated syntheses and characterization of CdSxSe1-x (x = 0, 0.25, 0.5, 0.75, 1) nanowires. The high quality crystallinity and optical properties of these nanowires were demonstrated for the potential optical sensor applications. The energy bandgap was also modulated by making solid solutions (CdSxSe1-x) in the spectral region from 1.74 eV to 2.45 eV as a function of the sulfur content. The photo-detector using CdSxSe1-x nanowires demonstrated well defined spectral responses depending on the bandgap energy of CdSxSe1-x nanowires.

15. SUBJECT TERMS
Semiconductor Materials, Nano-Materials, Inorganic/Organic Materials

16. SECURITY CLASSIFICATION OF:			17. LIMITATION OF ABSTRACT	18. NUMBER OF PAGES	19a. NAME OF RESPONSIBLE PERSON
a. REPORT	b. ABSTRACT	c. THIS PAGE			
unclassified	**unclassified**	**unclassified**	**Same as Report (SAR)**	**10**	

(4) Travel Expenses US$ 5,000

(5) Overhead charges US$ 20,000 (20% against total budget)

(6) Miscellaneous US$ 5,000

*Total US$ 100,000 (Half of the budget was provided by KIST)

Background

One-dimensional (1-D) nanostructures have been extensively studied due to their potential applications as the building blocks for fabricating nanometer-scaled electronic and optoelectronic devices [1-5]. Various semiconducting nanowires, nanorods, and nanotubes of single element, oxide, and compound semiconductors, have demonstrated successfully their potentials for nano-devices. For example, Si and Ge nanowires (E_g=1.1 ~ 1.2eV) have been studied for bottom-up approaches for nanoelectronics whereas wide-bandgap semiconductor nanowires (E_g=3.0 ~ 3.6eV), including ZnO and GaN, were also significantly investigated for the nano- optoelectronic applications.

The synthetic routes for nanowires and nanorods are basically based on the single crystal growth processes, such as Vapor-Liquid-Solid (VLS) process [4]. Thus, the crystal quality of the nanowires together with their optical and electrical properties are far better than those of thin films or bulk materials with same composition [1]. In this regard, the nanowires with wide bandgap could be good candidates for optical sensors, especially in the applications requiring better sensitivity and selectivity [6-7]. There are several merits in nanowire-based optical sensors when compared to thin film- or bulk- based sensors. Firstly, a far better sensitivity could be obtained due to their better crystallinity. In a reference, the nanowire-based sensors exhibit several tens times higher sensitivity compared to thin films or bulk materials with same compositions [6]. Also, there is a unique functionality of polarization sensitivity in nanowire- based optical sensors [7]. Although there have been several reports on the nanowire- based optical sensors [6~7], most of them are dealing with UV sensors based on wide-bandgap semiconductors.

Luminescence and fluorescence are typical outputs of various chemical and biological reactions or analysis. For an example, in the rapid test kits for immunoassay, luminescence or fluorescence are generated [12]. After a target sample (antigen, e.g. AIDS or cancer protein) reacts with a designated antibody (commercially available, e.g. Horseradish peroxidase), several enzymes are produced from the antigen-antibody reactions. The produced enzymes react with linker materials (commercially available, e.g. adamatane-dioxetane) and then generate luminescence or fluorescence of visible wavelength as the final output. These rapid test kits for immunoassay are widely used in medical “point-of-care” analysis, the annual worldwide market size being ~ 1 billion $. For this application, photodiode, PMT (photo multiplier tube), and CCD (charge coupled device) are usually used as the optical sensing devices [12]. If we use CdS_xSe_{1-x} nanowires as the optical sensing devices, however, better sensitivity and selectivity could be obtained due to their better optical / electrical properties and bandgap tunability. As we can control the energy bandgap in CdS_xSe_{1-x} nanowires, we can cut off the above- and below- band light. Thus, we could obtain better selectivity of the signal. Importantly, we can reduce the cost of test kits by using nanowires together with simple driving circuit, compare to CCD and PMT technology.

In this project, we have successfully synthesized CdS_xSe_{1-x} (x = 0, 0.25, 0.5, 0.75, 1) nanowires [8~10]. The high quality crystallinity and optical properties of these nanowires were good enough to be applied to optical sensors. Furthermore, their energy bandgap could be modulated by making solid solutions (CdS_xSe_{1-x}) in the spectral region from 1.74 eV to 2.45 eV as a function of the sulfur content [11]. The photo-detector using CdS_xSe_{1-x} nanowires demonstrated well defined spectral responses depending on the bandgap energy of CdS_xSe_{1-x} nanowires.

Experimental Results

(1) Synthesis of visible bandgap semiconductor nanowires

Figure 1 shows the hot-wall pulsed-laser deposition (PLD) sep-up used for the synthesis of visible bandgap semiconductor nano-structures using the complete solid solution of CdS and CdSe. From the preliminary experiments on the growth behavior, we found that the heater temperature (< 800°C) used in a typical stainless-steel chamber is not high enough to produce high quality epitaxial nanostructures. Thus, we designed a hot-wall quartz chamber enclosed by a tube furnace and controlled the target and substrate temperature up to 1100°C. A stoichiometric CdS_xSe_{1-x} (x = 0, 0.25, 0.5, 0.75, 1) targets were prepared by a cold pressing of CdS and CdSe powders (>99.9%, <1μm, Sigma-Aldrich) followed by a calcination at 1000°C for 2 hrs. CdS_xSe_{1-x} targets were ablated by KrF excimer laser (λ = 248nm) beam at the energy density of 1-4 J/cm^2 and at the repetition rate of 20Hz and then the target materials were transferred onto the surface of Au-coated Si (001) substrates.

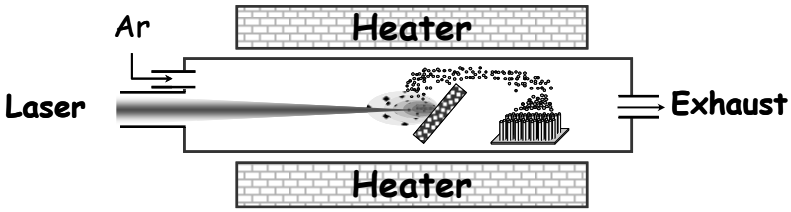

Figure 1. Hot-wall quartz PLD chamber designed in this study

Figure 2 shows the SEM images of various shapes of CdS_xSe_{1-x} nanostructures including nanowires, nano-ribbons, and nano-sheets. We could control the shapes of nanostructures by adjusting synthesis temperature, ambient pressure, and the flow rate of carrier gas. As seen in the figure, a large amount of random-oriented CdS, CdSe, and their solid solution nanowires with diameters of 50-200nm and a length of 10-50μm were synthesized. The insets of the figure shows detailed images of the tip part of the synthesized nanowires, which show alloyed tips of Au and CdS_xSe_{1-x} composition. As the Au catalyst was used in the synthesis, the deposited Au layer contributed to the formation Au-CdS_xSe_{1-x} eutectic alloying liquid, which enables the rapid growth of CdS_xSe_{1-x} nanostructures in a relatively low-temperature.

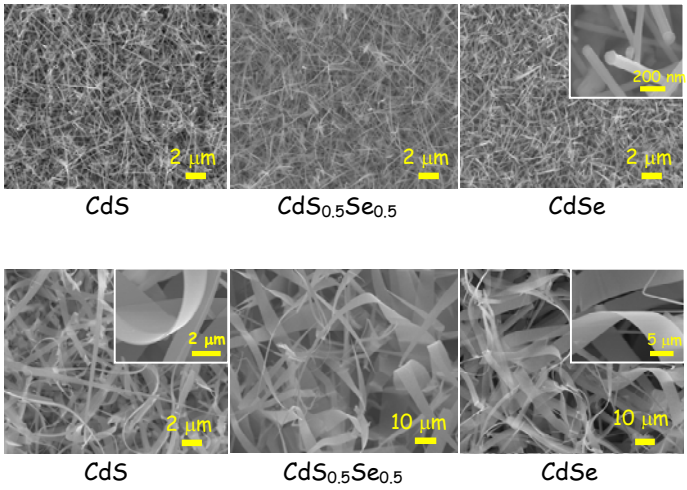

Figure 2(a). SEM images of CdS_xSe_{1-x} nanowire, nano-ribbon, and nano-sheets

Figure 3 illustrates the growth mechanism of nanowires and their evolution to nanoribbons or nanosheets by vapor-liquid-solid (VLS) and vapor-solid (VS) mechanism, respectively. In VLS mechanism, a liquid metal catalyst or Au in this study acts as the energetically favored site for absorption of gas-phase reactants. The Au-CdS_xSe_{1-x} eutectic liquid alloy supersaturates in CdS_xSe_{1-x} and 1-dimensional structures of CdS_xSe_{1-x} precipitates or grows beneath the eutectic liquid alloy. Thus, the thickness of nanowires is predominantly determined by the diameter of the liquid metal catalysts that can be achieved under equilibrium conditions (process A and B in the figure). Although the side facet of nanowires is energetically less favorable than the surface of Au-CdS_xSe_{1-x} liquid alloy tips, materials can still adsorbed on the side facet of the nanowires, which lead to the dendritic side branching through VS mechanism (process C). Dendritic crystals in homogeneous and epitaxial crystal growth are generally attributed to the diffusion-limited process in a supersaturated environment. For an example of ice-crystal, fern-like dendrites are initiated by the Mullins-Sekerka instability. In this case, the dendrites can be developed by the morphological instability via a VS growth mechanism without catalyst. So, the comb-like side-branching from the nanowire in this work appears to be related to the morphological instability in a supersaturated vapor environment. This explanation can be supported by the fact that dendrite structures are usually synthesized at higher temperature or higher supersaturation of the materials that that of nanowires. After completion of the dendritic side-branching, the nanostructure evolves to nano-ribbon or nano-sheets as in Fig. 2 (process D and E).

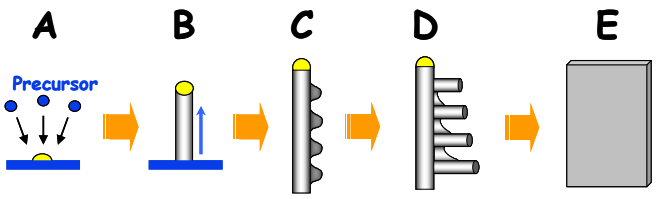

Figure 3. Evolution in the shapes of nanostructure from nanowire to nano-ribbon or nano-sheet

(2) Modulation of bandgap energy in CdS_xSe_{1-x} nanowires

Figure 4 shows the TEM images, selective-area electron diffraction (SAED) and the EDS results of several samples of the CdS_xSe_{1-x} nanowires. The diffraction patterns show that the growth direction of the CdS_xSe_{1-x} nanowires is aligned in the [001] direction. Atomic concentrations of Cd, S, and Se in the synthesized nanowires could be identified in the EDS analysis, as seen in the figure. For these qualitative and quantitative examinations, we could confirm that the CdS_xSe_{1-x} nanowires are a solid solution with a good single crystallinity.

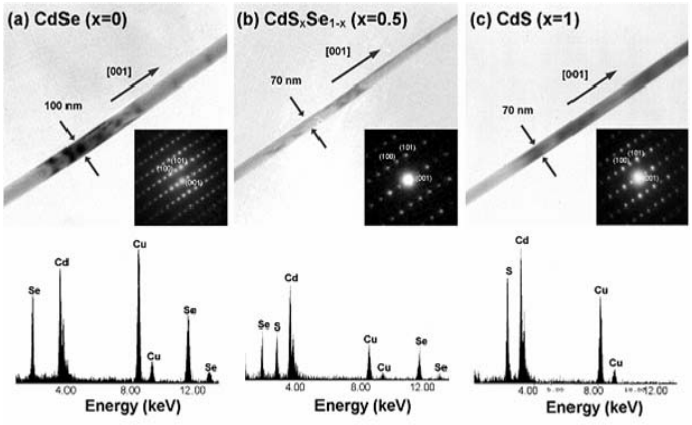

Figure 4. Bright-field TEM images with the inset of SAED patterns, and EDS spectrum of (a) CdSe, (b) $CdS_{0.5}Se_{0.5}$, and (c) CdS.

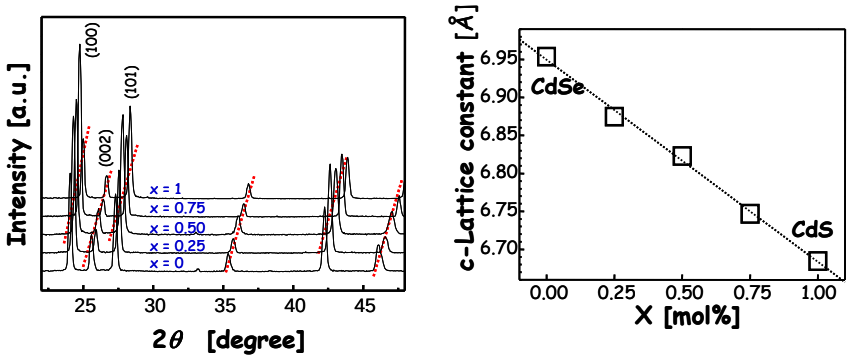

Figure 5. X-ray diffraction patterns of CdS_xSe_{1-x} alloy nanowires with different values of composition. The right figure is the calculated c-lattice parameters determined from (002) XRD peaks.

This excellent crystallinity could also be confirmed by the XRD patterns of the CdS_xSe_{1-x} nanowires, as shown in Fig. 5. The single phase of hexagonal structure was confirmed without any secondary phases in the whole composition range. XRD analysis indicates that the solid-synthesized CdS_xSe_{1-x} nanowires are a solid solution indeed. We also observed a shift in the peak position toward the higher angle with the increase of x content. The *a*- and *c*-lattice parameters determined from XRD peaks are summarized in Table 1. The *a*-axis and *c*-axis linearly decrease with the increase of x content in accordance with Vegard's law, which could be attributed to the larger size of Se substituted at the *a*-axis and *c*-axis of the

hexagonal crystalline structure.

Table 1. The *a*- and *c*-lattice parameters determined from XRD peaks.

	Unit cell volume (Å^3)	*a*-axis (Å)	*c*-axis (Å)
CdS	109.77	4.270	6.954
$CdS_{0.25}Se_{0.75}$	106.32	4.226	6.875
$CdS_{0.50}Se_{0.50}$	103.83	4.192	6.823
$CdS_{0.75}Se_{0.25}$	100.64	4.150	6.747
CdSe	97.76	4.110	6.685

The optical properties of the selected compositions of the CdS_xSe_{1-x} nanowires were characterized using the PL measurements. Figure 6 shows the PL spectra of the CdS_xSe_{1-x} nanowires with different values of x. the greater the value of x, the higher the energy corresponding to the peak of the near-band-edge emission. In other words, an increase in the value of x gives rise to a blue shift from 1.74eV (CdSe) to 2.45eV (CdS). In the previous work, the band gap of CdS_xSe_{1-x} films becomes larger with increasing x, and the PL peaks, corresponding to the highest intensity of the samples that matched well with these results. However, in this present work, the PL spectra of the CdS_xSe_{1-x} nanowires only have one band edge emission peak. We believe that this luminescence behavior of the nanowires is distinguished from the typical luminescence behavior of the case of CdS_xSe_{1-x} film from luminescence such as that which results from a defect involving structural disorder. These structural disorder defects were reported to be caused by vacancies. In particular, the PL peak becomes sharpened as a function of x. one of the reasons for the sharpening behavior of the PL peak with an increase in the value of x is that we can consider electronic scattering effects, which result in the variation in the width of the peak. Compared with the case of CdS (S with electronic orbital of 3s24p4), electronic scattering effects in CdSe (Se with electronic orbital of 4s24p4) would broaden the peak. We believe that this scattering-driven broadening of the PL peaks should be treated in an independent study involving other experimental cases examining PL characteristics of alloy nanowires.

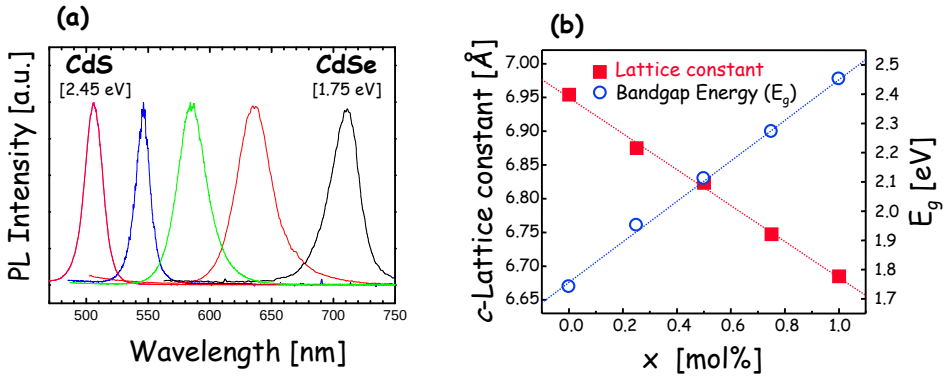

Figure 6. (a) Room-temperature PL spectra of CdS_xSe_{1-x} alloy nanowires as a function of x content. (b) Variation of the bandgap energy with composition of CdS_xSe_{1-x} alloy nanowires as a function of

x content with a linear fit.

(3) Fabrication of nanowire-based visible-range photo-detectors

Figure 6 illustrates the fabrication procedure of nanowire-based photo-detectors. First, nanowires, synthesized on a Si substrate (process a), were detached from the substrate by scratching with razor blade and suspended in IPA solution (process b) followed by ultrasonic treatment for better suspension. Second, the NW suspension was dispersed on the inter-digitized electrodes (IDT). One can see lots of nanowires networked between two electrodes (process c and d). We used transparent 0.5-mm thick, 4-inch Pyrex glass as a substrate. 800nm-thick SiO_2 layer was deposited by plasma-enhanced chemical vapor deposition (PECVD) on the substrate in order to avoid the possible contamination from the substrate. The IDT pattern was fabricated by Cr(10nm)/Au(50nm) metallization. Au was chosen for the contact metallization because of the well-known selective strong covalent bonding between Au and S in CdS_xSe_{1-x} nanowires. And finally, we deposited acrylates on top of the IDT with networked nanowires for device passivation (process e). Transmission of the passivation layer was found to be >95% at the wavelength of 400nm and the above, as seen in Fig. 7.

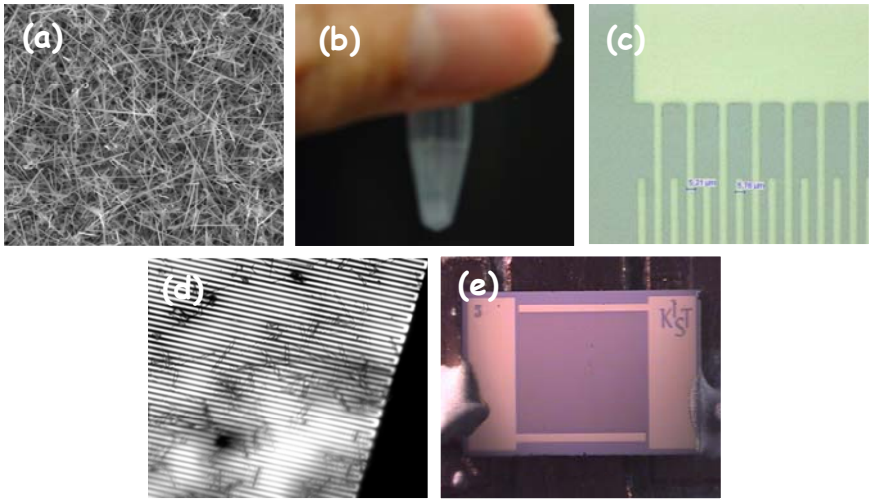

Figure 6. Fabrication procedure of nanowire-based photo-detector.

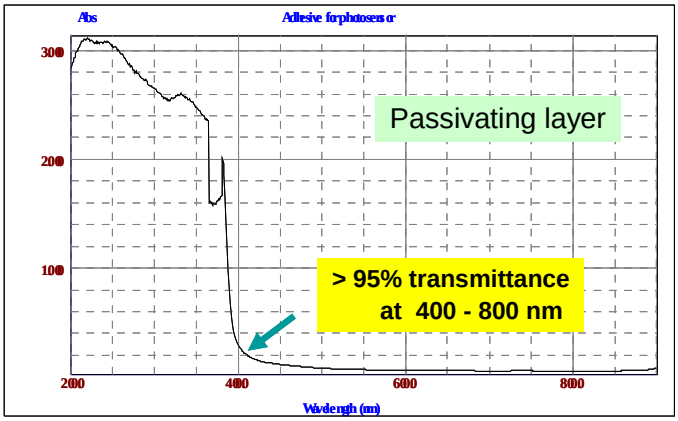

Figure 7. Optical property of the passivation layer.

Figure 8 shows the optical responses of CdS_xSe_{1-x} nanowires photo-detector as a function of wavelength ranging from 200nm to 900nm. The operation principle of photo-detector is to measure the change of the electrical conductivity depending on the intensity of illumination light. When a photon with higher energy than the bandgap of the semiconductor is incident, it can generate an electron-hole pair, which results in the increase of electrical conductivity. In the figure, one can clearly see the shift in the threshold wavelength towards longer wavelength region with increasing Se content. This observation is in good agreement with that in Fig. 6. This result indicates that the concept of bandgap energy modulation using the solid solution of CdS-CdSe can be successfully realized in nanowire-based photo-detector.

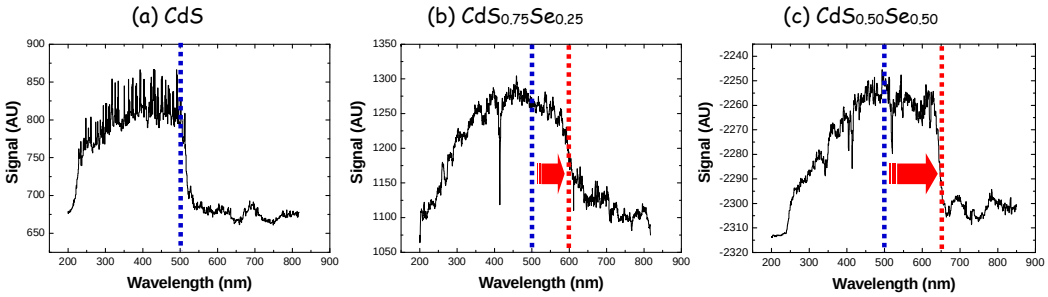

Figure 8. Opto-electronic property of CdS_xSe_{1-x} nanowires photo-detector.

Potential Applications

These kinds of tunable bandgap materials could be applied to various optical sensors, especially for the fluorescent probes in biological imaging, and spectroscopic analysis. For an example, CdS_xSe_{1-x} nanowires could be useful in fluorometric sensors as shown below. When we analyze samples (antigen), we could generated fluorescence or luminescence (typically, in the below figure, $\lambda 1$ = 490~650nm, $\lambda 2$ =520~700nm, $\lambda 3$ = 400~620nm) by tagging proper antibody and linker materials. In conventional technologies, photodiode, PMT, and CCD have been used as the optical sensing devices.

When we use CdS_xSe_{1-x} nanowires as the optical sensing devices, however, higher sensitivity and selectivity could be obtained due to their better optical/electrical properties and bandgap tunability. As we can control the energy bandgap in CdS_xSe_{1-x} nanowires, we can cut off the above- and below-band light. Thus, we could obtain better selectivity of the signal. Importantly, if we make the array of some CdS_xSe_{1-x} nanowires having different energy bandgap, we might analyze several kinds of samples simultaneously as we can detect several wavelengths.

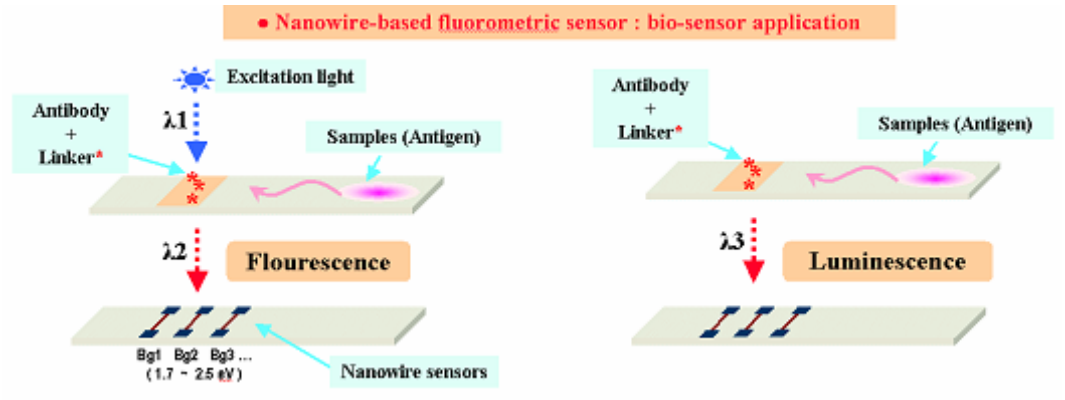

Figure 9. Nanowire-based fluorometric sensors

The second example is the nanowire-based spectroscopy, as shown below. Due to the bandgap tunability in CdS_xSe_{1-x} nanowires, we could identify the wavelength of the generated fluorescence light by making the array of some CdS_xSe_{1-x} nanowires having different energy bandgap. Eventually, we could identify the sample materials in micro channel. We can realize very small analyzing assembly by using nanowires rather than CCD and PMT. Furthermore, we could eliminate the optical filters as we can control the bandgap of the nanowires appropriately.

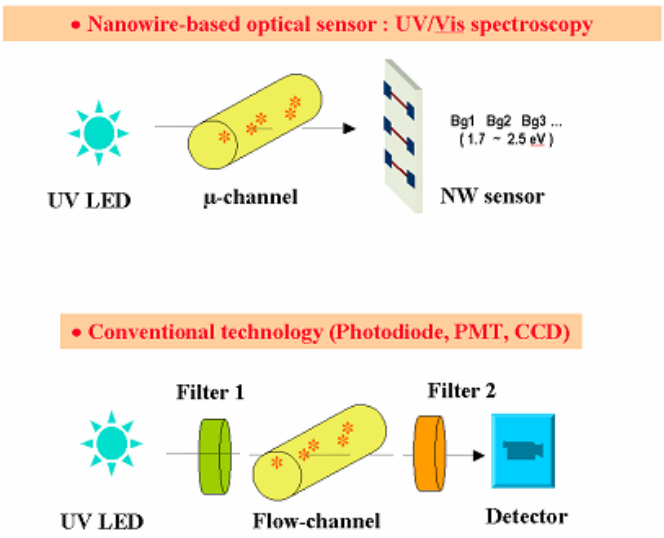

Figure 10. Nanowire-based spectroscopy and conventional technology

Publication

Paper

1. Band gap modulation in CdSxSe1-x nanowires synthesized by a pulsed laser ablation with the Au catalyst, *Nanotechnology* 17, 3775 (2006)
2. Optical properties of CdS nanowires, nanobelts, and nanosheets, to be submitted to *Applied Physics Letters*.

Presentation

1. Synthesis of CdSxSe1-x nanostructures and their optical properties, The 31st Annual Conference of the Korea Vacuum Society 2006
2. Synthesis and optical sensing characteristics of CdSxSe1-x alloy nanowires, IUMRS-ICA 2006
3. Band gap modulation of single crystalline CdSxSe1-x ternary alloy nanowires, IEEE Nanotechnology Materials and Devices Conference 2006

References

1. Y. Xia, Adv. Mater. **15**, 353 (2003).
2. Y. Cui, Science, **293**, 1289 (2001).
3. W. U. Huynh, Science, **295**, 2425 (2002).
4. M. H. Huang, Adv. Mater., **13**, 113 (2001).
5. X. Duan, Nature, **409**, 66 (2001)
6. H. Kind, Adv. Mater. **14**, 158 (2002)
7. J. Wang, Science, **293**, 1455, (2001)
8. Jae-Hwan Park, Heon-Jin Choi, Young-Jin Choi, Seong-Hyung Sohn, and Jae-Gwan Park, "Ultrawide ZnO nanosheets", Mater. Chem., cover illustration, **14**, 35 (2004).
9. Jae-Hwan Park, Heon-Jin Choi, Young-Jin Choi, Seong-Hyung Sohn, and Jae-Gwan Park, "Synthesis of ZnO nanorods by a hot-wall high-temperature laser deposition process", J. Cryst. Growth **276**, 171 (2005).
10. Jae-Hwan Park and Jae-Gwan Park, "Hierarchical evolution of arrayed nanowires, nanorods, and nanosheets in ZnO", Appl. Phys. A, **80**, 43 (2005)
11. Young-Jin Choi, In-Sung Hwang, Jae-Hwan Park, and Jae-Gwan Park, "Bandgap modulation in CdS_xSe_{1-x} nanowires synthesized by a pulsed laser ablation", Nanotechnology **17**, 3775 (2006).
12. K. Dyke, 1.Light Probes, in: Luminescence biotechnology, CRC Press, 2002.